

# Learning Contextualized Music Semantics from Tags via a Siamese Network

Ubai Sandouk, and Ke Chen

School of Computer Science, University of Manchester, Manchester M13 9PL, UK  
ubai.sandouk@manchester.ac.uk, chen@cs.manchester.ac.uk

## Abstract

Automatic annotation of music with tags is a promising methodology for the acquisition of semantics that facilitates music information retrieval and understanding. One of the biggest challenges for this methodology is modeling concept semantics in context. Moreover, the out of vocabulary (OOV) problem exacerbates its difficulty and has yet to be addressed so far. In this paper, we propose a novel Siamese network to fight off the challenge. By means of tag features and a probabilistic topic model, our Siamese network captures contextualized music semantics from tags via unsupervised learning, which leads to a contextualized music semantic space and a potential solution to the OOV. We have conducted simulations on two public tag collections, CAL500 and MagTag5K, and compared our approach to a number of the state-of-the-art methods. Comparative results suggest that our approach outperforms the state-of-the-art methods in terms of semantic priming measures.

## 1. Introduction

Music information retrieval is facing ever increasing challenges (Serra et al., 2013). In particular, the semantic gap between media and high-level annotations (Smeulders et al., 2000) has become the biggest difficulty in the natural understanding of music.

In efforts to bridge the music semantic gap, using direct mapping between music tracks and annotations (i.e. tags) has been a dominant approach (Bertin-Mahieux et al., 2010). However, this direct mapping adopts the tags independence assumption so that the relatedness among tags is not accounted for. More recently, a second mapping between the output of independent annotators and the tags has been introduced aiming to improve the annotation further. This is named “contextualized auto-tagging” (Miotto & Lanckriet, 2012). However, this method does not take actual tag-to-tag relatedness into account and learns only a refinement of the annotation. Due to a set of fixed tags used, direct mapping cannot deal with the out of vocabulary (OOV) problem; i.e. unseen tags in training appear in test.

Mandel et al., (2011) proposed a method for learning a track representation via “smoothing”. Smoothing learns the relationship between track’s information, e.g., track’s and users’ IDs, and the Bag-of-Words (BoW) representation of the track (Harris, 1954). To some extent, tag-to-tag relatedness is implicitly encoded in the learnt representation. As the new representation is learnt based on track features, the authors described their method as “contextualized tag inference”. However, their representation is simply used to improve the mapping between media and tags.

Motivated by language models used in natural language processing, we envisage a problem on *learning contextualized music semantics from tags*. In natural languages, context is reflected in the order of the words. Although music tags do not have such syntactic dependency, our observations suggest that we can still explore music tags context in a similar way. On one hand, some tags have a few intended meanings and are usually jointly used with others to indicate different musical concepts, e.g. ‘guitar’. On the other hand, different tags can have either the exact same meaning, e.g., ‘drums’/‘drumset’, or similar meaning in specific context, e.g., ‘techo’/‘electro’. Besides, there exists meaning overlapping, e.g., ‘orchestral’/‘classical’. Usually a music track is annotated by a set of tags, named *document* hereinafter. For a specific tag in a document, all tags in the document create its contextual niche which helps inferring the accurate intended meaning in this *local context*. As a result, the exploration of tag collections allows us to learn contextualized semantics; provided that tags of different uses indeed convey all musical concepts. This is a very difficult problem because a) tags get their meaning in groups, not in singularity; and b) it is unclear how to capture intrinsic context in tags. Nevertheless, solving this problem should bring us closer to bridging the semantic gap to improve music information retrieval and understanding.

In this paper, we propose a novel Siamese network (Bromley et al., 1993) to capture contextualized music semantics from tags. First of all, we extract a set of features from all tags available in order to form a raw tag representation. Then we employ a probabilistic topic model (PTM) to encode the local context of a tag’s use. Our Siamese network explores such information via unsupervised learning to establish a contextualized semantic space; this space embeds the different tags such that their semantic relatedness in context is reflected by their distances. As a result, our approach leads to multiple representations for a tag in different contexts so that it always co-locates with tags in its local context in the embedding space. Thanks to use of the tag features, our approach can accommodate OOV tags and hence leads to a potential solution to this problem.

The rest of the paper is organized as follows. Sect. 2 reviews the related work. Sect. 3 describes feature extraction and Sect. 4 presents our Siamese network and learning algorithm while Sect. 5 reports experimental results and the last section discusses relevant issues.

## 2. Related Work

In this section, we review related work in terms of learning music semantics from tags.

Levy and Sandler (2008) captured the dependence of tags using Latent Semantic Indexing (LSI) (Deerwester et al., 1990). LSI relies on generating a tag-to-tag relatedness by analyzing the entire document-tag matrix to uncover patterns of collective use of tags. Aside from their poor generalizability to new tags as well as to new documents, the semantics captured by LSI are non-contextualized. This means that the relatedness between any pair of tags is always the same regardless of context. Hereinafter, this type of semantics is referred to as “global relatedness”.

As opposed to the global semantics, topic models implicitly address the locality by introducing the topic concept. Topics are latent concepts that capture correlation among observed tags. Probabilistic Latent Semantic Analysis (P-LSA) (Hofmann, 1999) and Latent Dirichlet Allocation (LDA) (Blei et al., 2003) are the most prominent topic models used in natural language processing. Technically, they model topics as distributions over tags and provide a summary of each document in the form of a distribution over topics. However, those topic models fail to account for the global relatedness between the tags and thus can only provide ad-hoc tag-to-tag relatedness. In addition, they are not able to deal with the OOV problem.

Mandel et al., (2011) proposed a novel document representation method named smoothing which is contextualized based on available information regarding documents and users. Smoothing provides a concise representation of tags’ relevance for each document via representation learning on the level of documents. The representation is used in learning track to tag mapping. Therefore, it is an effort working towards bridging the semantic gap. However, their method does not consider contextualized relatedness measures and cannot handle the OOV problem. In addition, the learnt semantics are limited to the mapping task because the method works on the document representation level.

Distributed language models (Mikolov et al., 2010; Collobert et al., 2011; Mikolov et al., 2013) have recently been attracting increasing attention due to their simplicity and capacity in providing generic semantics for later tasks (Frome et al., 2013; Mikolov et al., 2013). Such models yield a semantic space where all words are embedded properly based on their contextualized syntactic similarity (Mikolov et al., 2010). Natural language processing benefits from such technique as the context is naturally present in the syntactic structure. Nevertheless, applying such technique in the tag domain seems unrealistic due to the lack of syntactic structure among tags.

Other language models may relax the syntax structure requirement by concentrating on the co-occurrence events of different words. By careful preprocessing of the document-word matrix, a linear model based on PCA has been shown to capture the word-to-word relationship well (Lebret et al., 2013). Still, such models are sensitive to preprocessing and could potentially be enhanced using other techniques, e.g. different aggregation measures (Markines et al., 2009). When this model is applied to music tags, it is only able to capture the global relatedness.

In summary, the existing work does not sufficiently address issues on the contextualized music semantics learning from tags.

### 3. Tag and Local Context Representations

To facilitate the presentation of our proposed Siamese network, we describe the input representation required by our approach. The input consists of features of a single tag concatenated with features of its local context.

In general, tags can be characterized by either ID-based or statistics-based representations. An ID-based representation uses a scheme directly linked to the tag’s ID, e.g., BoW. A statistics-based representation uses statistical analysis of the use of the tag within the dataset. The major drawback of ID-based representations lies in its ordinal nature as well as their limited ability to represent OOV tags. In contrast, statistics-based representations inherently overcome these limitations. In our approach, we employ a statistics-based representation adapted from the works (Markines et al., 2009; Singhal, 2001) so that a tag can be represented based on its use regardless of its presence in training. In this representation, we first re-weight the document-tag matrix using *tfidf* as defined below. Then we aggregate pairs of tags using dot product. Given a single tag  $\tau$  from a set of possible tags  $\Gamma$  and a single document  $\delta$  from the set of known documents  $\Delta$ , the tag frequency in that document  $tf(\tau, \delta)$  is defined as:

$$tf(\tau, \delta) = \begin{cases} 1 & \text{when } \tau \text{ appears in } \delta \\ 0 & \text{otherwise} \end{cases}.$$

The rarity of tags in the collection is accounted for by the inverted document frequency  $idf(\tau)$ :

$$idf(\tau) = \log \left( \frac{|\Delta|}{1 + |\{\delta: \tau \text{ appears in } \delta\}|} \right),$$

where  $|\cdot|$  is the cardinality of a set.

The *tfidf* weights are defined as the product of the tag frequency and the inverted document frequency:

$$tfidf(\tau, \delta) = tf(\tau, \delta) \times idf(\tau).$$

For aggregation, the usage of tag  $\tau$  over all documents is characterized by all of its *tfidf* values and denoted by  $\mathbf{u}(\tau) = \{tfidf(\tau, \delta_i)\}_{i=1}^{|\Delta|}$ .

The global relatedness between two tags  $\tau_1$  and  $\tau_2$  is measured by their usage vectors dot product:

$$T(\tau_1, \tau_2) = \langle \mathbf{u}(\tau_1), \mathbf{u}(\tau_2) \rangle$$

As a result, a tag is represented by  $|\Gamma|$  features denoted by

$$\mathbf{t}(\tau) = \{T(\tau, \tau_i)\}_{i=1}^{|\Gamma|}. \quad (1)$$

Based on the used measures, we call this pre-processing technique “*tfidf+dot-product*”. For an OOV tag, its *tfidf* value can be measured as same as done for in vocabulary tags. However, the aggregation is only done against known tags. This setting ensures the same number of features is used to represent both known and OOV tags. In addition, each feature always means relatedness against the same tag. Hence, such tag features provide a potential solution to the OOV problem provided that OOV tags co-occur with known tags.

By considering all the tags co-occurring in the same document as local context of any tag in this document, we also face a representation problem. An ideal context representation is semantically consistent across documents and easy to estimate within application, e.g. music annotation. Motivated by recent work where a model was trained to predict topic distributions directly from acoustic features (Law et al., 2010); we use the LDA (Blei et al., 2003) to model the local context. The LDA model assumes a set of independent topics  $\Phi$  that softly cluster the documents based on the used tags. While training, the process learns scalar priors  $B$  for Dirichlet distributions which are used to model the topics. After training, given a tag  $\tau$  in a specific document  $\delta$ , the posterior probability of any topic  $\phi \in \Phi$  follows  $p(\phi|\tau) \sim p(\tau|\phi)p(\phi)$ , where  $p(\tau|\phi) \sim \text{Categorical}(\phi)$  and  $p(\phi) \sim \text{Dirichlet}(B)$ . Moreover, the posterior topic probability of one document  $\delta$  consisting of tags is:

$$p(\phi|\delta) \sim p(\phi) \prod_{\tau \in \delta} p(\tau|\phi).$$

As a result, a document as a local context is represented by  $|\Phi|$  features denoted by:

$$\mathbf{l}(\delta) = \{l_c(\delta)\}_{c=1}^{|\Phi|}, \quad l_c(\delta) = p(\phi_c|\delta). \quad (2)$$

## 4. Model Description

As required by music information retrieval applications, our model is built to represent solitary tags. Nonetheless, the accurate meaning of a tag’s use cannot be determined unless the local context is taken into account. As a result, the same tag in different documents may have different meanings. On the other hand, different tags may share the same meaning in similar local contexts. Unlike learning global relatedness where each tag has a unique meaning, we encounter a more complex semantic learning problem. To deal with it, we propose a Siamese network and learning algorithms for modeling music concept semantics by considering tags and local contexts simultaneously.

### 4.1. Architecture

As illustrated in Fig. 1, the proposed architecture consists of two identical component networks. Each is a feed-forward neural network of  $H$  hidden layers. The input consists of features of a tag and its local context, while the output is the estimated binary Bag of Words (BoW) representation of the document in question. Two networks are coupled and trained via two-stage learning presented in Sect. 4.2.

To make an initial semantic embedding, one component network is trained to infer the BoW of a document from input features of a tag and its local context. After this learning, the output of the  $(H - 1)^{\text{th}}$  hidden layer is used as an initial contextualized semantic representation given a tag in a certain local context. We refer to this representation as *contextual embedding* (CE) throughout the paper. While a component network can embed the coherent tags in a document properly, this initial semantic embedding may not fully meet the requirements of co-location of all relevant tags in similar contexts.

To make the proper embedding, we couple two identical component networks and revise the initial semantic embedding via *contrastive learning* working on further constraints. During the contrastive learning, two networks work together to deal with different situations regarding all possible types of input. As regularization, each component network is still trained simultaneously to infer the BoW in order to avoid unnecessary changes of learnt semantics in the initial embedding stage.



$$\mathcal{L}_P(X; \Theta) = -\frac{1}{2K|\Gamma|} \sum_{k=1}^K \sum_{j=1}^{|\Gamma|} (\kappa_k(1 + y_{kj}) \log(1 + \hat{y}_{kj}) + (1 - \kappa_k)(1 - y_{kj}) \log(1 - \hat{y}_{kj})) \quad (3)$$

$\kappa_k = \frac{|\{j: y_{kj}=1\}_{j=1}^{|\Gamma|}|}{|\Gamma|}$  is used to highlight the cost of a false negative, and  $K$  is the number of all training examples.

After completing the prediction learning, we train a Siamese network by coupling two copies of the trained network. Presenting a pair of input vectors  $\mathbf{x}^{(1)}, \mathbf{x}^{(2)}$  to the two component networks, the embedding similarity is defined by the Euclidean distance between their CE representations:

$$E(\mathbf{x}^{(1)}, \mathbf{x}^{(2)}) = \|\mathbf{CE}(\mathbf{x}^{(1)}) - \mathbf{CE}(\mathbf{x}^{(2)})\|_2.$$

The semantics are learnt by encouraging this distance to follow expected distance trends while conserving as much of the prediction ability as possible. For example, two different tags used to describe the same musical concept share identical local contexts and hence should have a zero distance. In contrast, a tag with two different meanings appears in at least two different contexts and its two representations should be significantly distant. Measuring contexts similarity depends on the local context via Kullback–Leibler (KL) divergence:

$$KL(\mathbf{x}^{(1)}, \mathbf{x}^{(2)}) = \sum_{c=1}^{|\Phi|} \left( (l_c^{(1)} - l_c^{(2)}) \log \left( \frac{l_c^{(1)}}{l_c^{(2)}} \right) \right).$$

The mentioned expected trends are represented as constraints considering the different cases. Let  $I_1, I_2$  and  $I_3$  denote the three cases of an input pair  $(\mathbf{x}^{(1)}, \mathbf{x}^{(2)})$ : 1)  $I_1 = 1$ : both are positive and embedding similarity should follow the trend of contexts similarity; 2)  $I_2 = 1$ : both are negative and embedding similarity should follow the trend of contexts similarity; and 3)  $I_3 = 1$ : one example is positive while the other is negative and the embedding distance should be maximized. The more similar the contexts, the more critical this case becomes.

Given two subsets  $X^{(1)}$  and  $X^{(2)}$  of the same cardinality  $N$  of randomly selected examples via pairing from the training set  $X$ , the Siamese loss is defined by

$$\mathcal{L}_S(X^{(1)}, X^{(2)}; \Theta) = \sum_{n=1}^N \left( I_1 \left( E(x_n^{(1)}, x_n^{(2)}) - \beta \left( 1 - e^{-\frac{\lambda}{2} KL(x_n^{(1)}, x_n^{(2)})} \right) \right)^2 + I_2 \left( E(x_n^{(1)}, x_n^{(2)}) - \beta \left( 1 - e^{-\frac{\lambda}{2} KL(x_n^{(1)}, x_n^{(2)})} \right) \right)^2 + I_3 \left( E(x_n^{(1)}, x_n^{(2)}) - \beta \right)^2 e^{-\frac{\lambda}{2} KL(x_n^{(1)}, x_n^{(2)})} \right). \quad (4)$$

Here  $\beta$  is a scaling factor used to ensure controlled tag spread over the embedding space.  $\rho < 1$  is an importance factor which allows the training to emphasis on the first case.  $\lambda$  is a sensitivity factor that affects to what degree the embedding similarity is dominated by the context similarity; the smaller, the more sensitive it is.

By combining losses defined in Eqs. (3) and (4), the total loss used in the second learning stage is

$$\mathcal{L}(X^{(1)}, X^{(2)}; \Theta) = \sum_{i=1}^2 \mathcal{L}_P(X^{(i)}; \Theta) + \alpha \mathcal{L}_S(X^{(1)}, X^{(2)}; \Theta). \quad (5)$$

$\alpha$  weighs the contribution of the Siamese cost.

Parameter estimation is done iteratively via stochastic back-propagation (SBP). In each iteration, a small batch of examples is randomly selected to update the parameters. After each iteration, the component networks are made identical by averaging their weights and biases. Details of our learning algorithms and their derivation can be found in Sect. A of the supplementary materials.

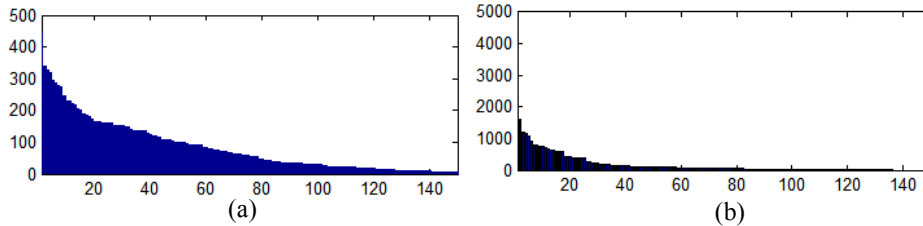


Figure 2: Frequency of tags used in all the documents in a dataset. (a) CAL500. (b) MagTag5K.

## 5. Experiment

### 5.1. Dataset and Feature Extraction

We employ two publically available datasets, *CAL500* (Turnbull et al., 2007) and *MagTag5K* (Marques et al., 2011), in our experiments. *CAL500* is a dataset of 500 documents annotated using 158 tags via surveys. The dataset is dense with average 25 tags per document. Additionally, the dataset lessen the effect of the long-tail by using the set tags. *MagTag5K* is a controlled version of MagnaTune where repeats and contradictions were removed. MagnaTune is the result of an online annotation game that allows the users to evaluate the appropriateness of complete sets of tags rather than one tag at a time (Law et al., 2009). *MagTag5K* contains 5,259 documents and 136 tags. It is much sparser than *CAL500* with average five tags per document. Fig. 2 clearly illustrates the difference in tag use between the two datasets.

For feature extraction, we achieve 158 and 114 tag features for *CAL500* and *MagTag5K* by applying the aggregation method described in Sect. 3, respectively. In addition, we empirically sought the number of topics in LDA by using the hierarchical process suggested in (Teh et al., 2006); 25 and 19 topics were used to represent local contexts in *CAL500* and *MagTag5K*, respectively.

### 5.2. Experimental Setting

All available documents and tags were used in our experiments. 22 randomly selected tags from *MagTag5K* were reserved for the OOV evaluation along with all the documents using them. Because of the density of *CAL500*, reserving a single tag for OOV evaluation would result in 160 documents unusable on average. For this reason, we refrained from OOV evaluation on *CAL500*. The remaining documents are split into two subsets for training and test in three-fold cross-validation.

Determining the hyper-parameters is done using grid search. Through the cross-validation, we found a proper network structure:  $input \rightarrow 100 \rightarrow 100 \rightarrow 10 \rightarrow output$  where  $\lambda = 0.5$  and  $\beta = 3$  were used for both datasets and  $\alpha = 2000$  and 1000 were set for *CAL500* and *MagTag5K*, respectively. Details on the parameter setting and model selection can be found in Sect. B of the supplementary materials.

For evaluation, we use the *semantic priming*. Priming is the ability to correctly rank all tags according to their semantic similarity to a query tag (Ferrand & New, 2003). Successful priming means that all related tags can be found before reaching any non-related ones.

For such a retrieval task, a model is assessed by measuring the performance of retrieving the top  $k$  tags in response to a query tag. Given that  $\mathbf{r}$  is the retrieved ordered list of tags and  $\bar{\mathbf{r}}_k$  is the ordered list composed of the first  $k$  tags of  $\mathbf{r}$ , precision at  $k$  is defined by

$$P@k(k; \delta, \mathbf{r}) = \frac{|\delta \cap \bar{\mathbf{r}}_k|}{k}.$$

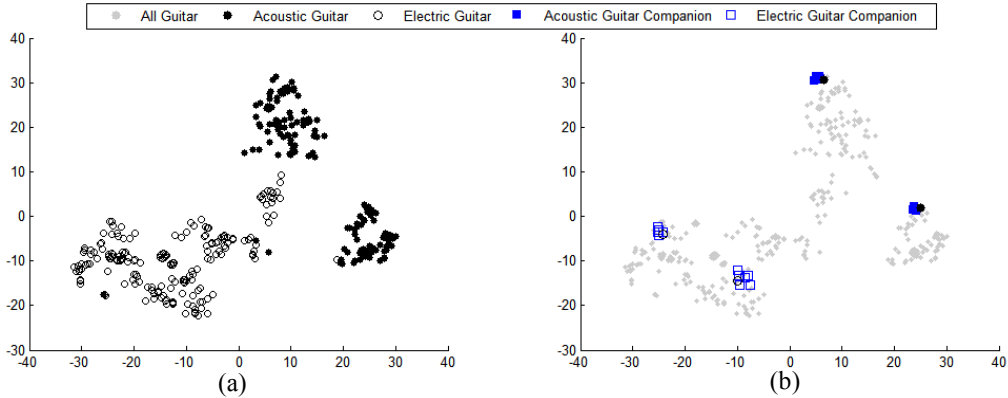


Figure 3: 2D projection of semantic representations of ‘Guitar’ and related tags in MagTag5K. (a) All 388 different guitar instances. (b) Randomly selected ‘Guitar’ instances with contextualized related tags.

The performance over the entire retrieved list is accessed by measuring the minimum numbers of retrieved tags required to achieve the standard 11 recall levels: 0, 0.1, 0.2, ..., 1 and their corresponding precision values (Manning et al., 2008, pp. 158–163). Precision and recall are measured as

$$Recall(\delta, \bar{r}) = \frac{|\delta \cap \bar{r}|}{|\delta|}, \quad Precision(\delta, \bar{r}) = \frac{|\delta \cap \bar{r}|}{|\bar{r}|}.$$

As a figure of merit, precisions corresponding to the top  $m$  levels are averaged for each query and the averages are aggregated to form mean average precision ( $MAP$ ).  $m$  is fixed over all test queries and is larger than average  $|\delta|$ . Another figure of merit is extracted by measuring area under curve the precision-recall curve ( $AUC$ ).

All those results are then aggregated over the entire set of queries. The  $P@k$  results are averaged at each level. Similarly, precision is averaged at each recall level, and  $MAP$  is directly averaged over the entire query set. As the ground truth lists to be retrieved have varying lengths,  $MAP$  better reflects the performance of a real application.

The OOV examples consist of OOV tags in their contexts. Due to the nature of LDA, only in-vocabulary tags were used to train the LDA. Once input is obtained for OOV examples, we query the model in a similar manner to the in-vocabulary case and measure the priming ability of each OOV tag in context. All the primed tags returned by an OOV query are in-vocabulary tags.

For thorough evaluation, we also compare our approach to the state-of-the-art approaches reviewed in Sect. 2, including LSI and p-LSA (Levy & Sandler, 2008), PCA (Lebret et al., 2013), Information Theoretic Smoothing (*InfoTh*) and Conditional Restricted Boltzmann Machine Smoothing (C-RBM) using one hot representation for the condition (Mandel et al., 2011), LDA (Law et al., 2010), and two natural language models: Continuous Skip-Gram (C-SG) and Continuous Bag-of-words (C-BoW) (Mikolov et al., 2013). As the RBM (Hinton, 2010) can inherently model the global relatedness of tags without the need for feature tuning, we also evaluated the RBM trained using the BoW representation on the visible layer. Additionally, we report the results of the random model, which retrieve tags randomly for any query. Our model is represented in two forms: the single component trained (Single CE) and the fully trained (Siamese CE).

### 5.3. Visualization

By using the unsupervised t-SNE (Maaten & Hinton, 2008), we project the embedding vectors regarding the tag ‘Guitar’ used in the dataset MagTag5K onto a 2D plane for visualization. As shown in Fig. 3(a), three clusters emerge. Based on the genres of the documents, we find that two clusters (●) are associated with documents of acoustic nature and the third (○) links to documents of electric nature. Fig. 3(b) illustrates the projection of all tags from four randomly chosen documents concerning ‘Guitar’ superimposed on all the ‘Guitar’ projections (shaded). It is seen that the companion tags (□, ■) are locating near the original ‘Guitar’ instances. This visualization demonstrates how different meanings of a tag are captured based on intention of use, rather than their mere co-occurrence. More visualization can be found in Sect. D of the supplementary materials.

METHOD	TRAINING					TEST				
	@1	@2	@5	@10	MAP	@1	@2	@5	@10	MAP
RANDOM	100±0.00	58.15±0.38	33.06±0.15	24.69±0.07	28.95±0.06	100±0.00	57.98±0.38	33.11±0.15	24.63±0.07	29.00±0.21
C-BOW	100±0.00	69.52±1.62	48.75±1.5	40.27±1.24	42.12±1.06	100±0.00	68.91±1.59	47.76±2.26	39.26±1.68	41.20±1.44
SG	100±0.00	70.11±1.52	49.04±1.25	39.07±1.45	41.22±0.75	100±0.00	69.76±2.16	48.40±1.20	38.24±0.45	40.55±0.49
LSA	100±0.00	76.24±0.87	57.66±1.62	49.34±1.69	50.74±1.55	100±0.00	75.33±1.47	56.09±1.48	47.70±1.48	49.32±1.06
LDA	99.95±0.08	78.7±0.1	61.09±0.25	51.00±0.86	52.18±0.65	99.97±0.05	76.62±0.69	58.02±1.45	47.99±1.29	49.29±1.11
P-LSA	100±0.00	78.09±0.59	60.11±0.38	49.73±0.35	49.96±0.71	100±0.00	75.90±0.71	56.50±1.45	45.75±1.94	46.35±1.06
PCA	100±0.00	80.72±0.71	65.21±0.81	56.35±0.72	56.69±0.46	100±0.00	79.78±0.68	63.92±0.96	54.89±0.85	55.39±0.74
RBM	87.60±1.15	80.20±0.40	69.95±0.20	62.19±0.32	61.26±0.51	88.47±3.25	77.00±2.53	67.02±1.82	59.27±1.46	57.77±0.79
INFOTh	100±0.00	83.00±0.00	68.08±0.00	59.36±0.00	59.31±0.31	100±0.00	<b>81.59±0.44</b>	66.31±0.27	57.71±0.47	57.69±2.01
C-RBM	88.30±0.00	82.20±0.44	76.64±0.27	68.11±0.47	65.83±0.00	N/A	N/A	N/A	N/A	N/A
SINGLE CE	100±0.00	88.20±0.80	79.48±1.22	76.35±1.21	76.98±0.18	100±0.00	80.13±1.18	67.24±1.86	62.10±2.28	63.34±2.23
SIAMESE CE	100±0.00	<b>91.57±1.40</b>	<b>84.89±1.24</b>	<b>82.73±1.56</b>	<b>84.87±1.36</b>	100±0.00	80.40±1.45	<b>67.51±2.30</b>	<b>63.01±2.43</b>	<b>64.33±0.78</b>

Table 1. Priming accuracy (%) of different approaches at different levels on CAL500.

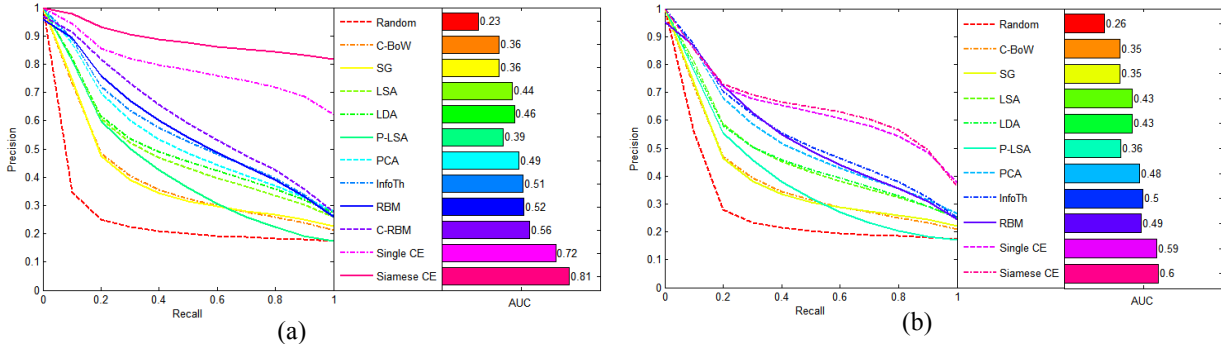


Figure 4: AUC results for different models on CAL500. (a) Training. (b) Test.

5.4. Results on CAL500

Table 1 lists the priming and MAP results of different models on CAL500. For a model, given a query tag, the first primed tag may be the query tag itself, generating a 100% accuracy in  $P@1$ . The evaluated natural language models generally perform poorly except for PCA. On the other hand, Smoothing improves the priming by augmenting the relatedness of tags. C-RBM has no testing results due to the capacity limitation of the model. It is evident from Table 1 that our model outperforms all others (p-value < .05, Student's t-test). It is also observed that the accuracy of some models does not drop sharply on longer retrieved lists; RBM, C-RBM and ours retain higher accuracies @10 than others. Moreover, the MAP results confirm the capability of our model in priming all related tags before reaching unrelated tags.

When testing on CAL500, we observe that there is a difficulty in priming the first few tags and hence the performance of all the models degrades as suggested by the MAP results. In order to better understand the nature of this case, we show the precision-recall curves in Fig. 4. In contrast to the training performance shown in Fig. 4(a), the retrieval of the first 10% related tags reduces precision more than the later tags in most models during test as seen in Fig. 4(b). This is also reflected in their AUC. However, ours is compensating on longer retrieved lists and with the improved AUC as observed in Fig 4(b).

METHOD	TRAINING					TEST				
	@1	@2	@5	@10	MAP	@1	@2	@5	@10	MAP
RANDOM	100±0.00	52.12±0.08	23.35±0.19	13.73±0.11	47.9±0.59	100±0.00	52.06±0.26	23.29±0.30	13.71±0.28	47.89±1.20
C-BOW	100±0.00	61.13±1.94	34.58±1.30	23.31±0.37	56.71±0.61	99.93±0.12	61.17±3.36	34.12±2.86	22.69±2.58	56.47±1.18
SG	100±0.00	61.55±1.59	35.60±1.07	24.01±0.36	57.54±1.08	99.93±0.12	61.59±4.74	35.18±4.40	23.32±3.15	57.34±2.95
LSA	100±0.00	58.25±1.13	33.05±0.81	22.10±1.05	54.98±0.94	100±0.00	58.02±2.04	32.49±2.73	21.14±1.60	54.58±0.66
LDA	100±0.00	65.54±0.59	35.84±0.75	21.23±0.67	58.3±0.09	100±0.00	65.52±1.23	35.81±1.56	21.20±1.38	58.30±0.18
P-LSA	100±0.00	64.94±2.18	34.75±2.36	19.76±1.71	57.95±1.49	100±0.00	64.23±3.05	34.18±1.50	19.34±1.08	57.41±0.90
PCA	100±0.00	69.15±0.70	41.63±1.29	28.28±1.05	62.86±0.33	100±0.00	68.26±2.36	40.59±2.67	27.46±1.99	62.00±1.08
RBM	65.53±0.00	58.60±0.08	43.81±0.19	32.15±0.11	54.22±1.55	25.87±0.00	19.92±0.26	17.53±0.30	16.73±0.28	20.84±4.57
INFOTh	99.75±0.03	73.03±2.14	46.18±2.71	32.04±2.09	66.44±1.55	100±0.00	71.44±3.04	44.9±3.80	31.05±3.29	65.18±2.25
C-RBM	74.93±0.00	67.02±0.00	48.09±0.00	33.66±0.00	60.03±0.00	N/A	N/A	N/A	N/A	N/A
SINGLE CE	100±0.00	86.23±0.21	71.65±0.60	49.57±1.70	85.60±1.37	100±0.00	82.83±2.59	64.69±6.08	43.50±4.46	79.97±2.07
SIAMESE CE	100±0.00	<b>88.33±0.50</b>	<b>75.49±1.72</b>	<b>54.14±1.34</b>	<b>86.89±1.50</b>	100±0.00	<b>82.70±1.57</b>	<b>67.57±3.42</b>	<b>46.30±2.55</b>	<b>81.16±2.31</b>

Table 2. Priming accuracy (%) of different approaches at different levels on MagTag5K.

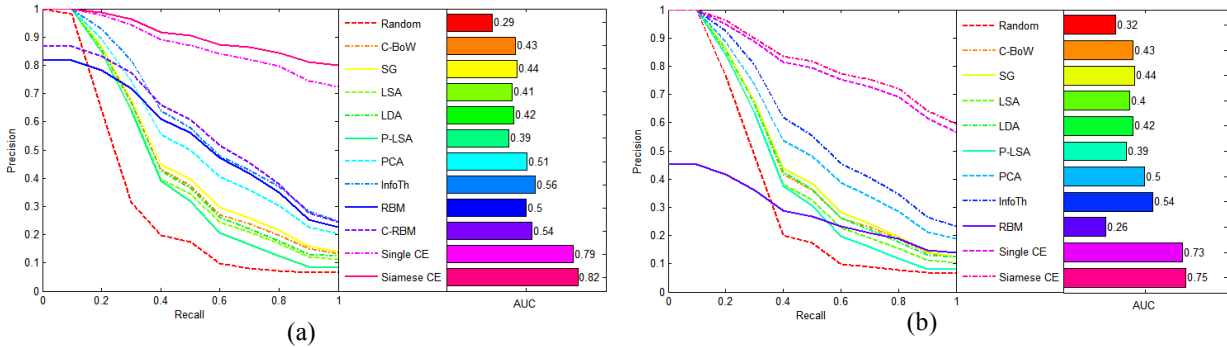


Figure 5: AUC results for different models on MagTag5K. (a) Training. (b) Test.

## 5.5. Results on MagTag5K

Table 2 lists the performance of all the models on MagTag5K. Due to its sparsity, most models perform worse than on CAL500. In contrast, ours performs well on both training and test. Our results here are consistent with those by the smoothing reported in (Mandel et al., 2011) and by the language models in (Lebret et al., 2013). Particularly, ours considerably outperform all others by gaining at least 32.8% and 24.6% higher accuracy in terms of MAP.

It is also observed from Fig. 5 that where most models struggle after retrieving 10% related tags, but ours does not. These results suggest that our model learns the semantic relatedness regardless of the sparsity.

## 5.6. Out of Vocabulary Results

After training, OOV tags are used to evaluate priming. OOV tags have input features based on the aggregation method described earlier. However, they are not used in training the local contexts. When testing, our approach has to assign any OOV tags to the negative example category, which leads to the collocation of OOV tags with those negative examples used in learning in the CE space. As OOV tags were pushed as far away as possible from all positive examples in the CE space, we stipulate that for an OOV tag its most related in-vocabulary tag is the one furthest in distance. As a result, Table 3 lists the priming results of ours and two other models that can handle OOV. It is evident that ours performs better than others the performance is degraded.

Learning Contextualized Music Semantics from Tags via a Siamese Network

METHOD	@1	@2	@5	@10
RANDOM	4.12 ± 0.00	4.21 ± 0.00	3.97 ± 0.00	4.00 ± 0.00
PCA	18.63 ± 0.74	18.77 ± 10.73	9.22 ± 6.04	8.56 ± 4.78
SINGLE CE	56.87 ± 1.80	55.17 ± 1.910	44.79 ± 2.28	28.14 ± 1.86
SIAMESE CE	<b>63.47 ± 2.57</b>	<b>62.9 ± 4.18</b>	<b>53.05 ± 3.94</b>	<b>33.21 ± 2.18</b>

Table 3. Priming accuracy (%) the OOV experiments.

## 6. Discussion

Unlike previous approaches in semantics learning, ours learn distributed semantics with no target task in hand. This should bring us closer to bridging the semantic gap encountered by various music related tasks. By considering local context, our approach leads to distributed multi-representations of a tag as is associated with semantically different contexts. These features significantly distinguish ours from others in music semantic embedding learning from tags.

“Tag ontologies” have already been used for capturing semantics (Kim et al., 2008; Wang et al., 2010). In contrast to our approach, tag ontologies require expert annotation of the tags and their relatedness. Moreover, it is much more difficult in creating ontologies on the contextualized semantic relatedness. In contrast, our approach learns such relatedness automatically from data in an unsupervised manner and can accommodate some unknown or non-standard tags, e.g., “r’n’b”, “alt”, “lo-fi”, “4ad”, “90s”. Thus, it becomes possible to handle OOV tags without introducing placeholders or ‘rare’ tokens.

Unlike those approaches to music semantic embedding learning based on various resources (Chen et al., 2012; Serra et al., 2013; Turnbull et al., 2009; Weston et al., 2011), our semantic embedding learning solely relies on tag collections. On the hand, our methodology allows us to avoid unnecessary complexity incurred by other possibly noisy resources. On the other hand, ours may face the problem of limited information available from the training datasets.

Exploring deep semantics in tags demands a powerful context model that can capture sufficient contextualizing information. Our choice of the PTMs in this paper acts as a generic tool for information aggregation from a document. However, PTMs have already been criticized for lack of interpretability, which subsequently renders the results of our model not interpretable. For a specific application, it may be suitable to use alternative context models such as labeled LDA (Ramage et al., 2009) trained with genre, emotion or instrument annotations as topic labels if those annotations are available. Likewise, user’s information may be used as context in order to provide personalized semantics in related applications. As a result, our approach is flexible in context representation.

In conclusion, we present a novel approach to learning contextualized music semantic representations from tags. While the work presented in this paper is only regarding the semantic embedding learning from tags, the representation generated by our approach may be applied to various music information retrieval tasks, e.g., auto-annotation of music tracks by mapping from the acoustic features onto the embedding space, semantic music retrieval by using our embedding representations as indexing terms and facilitating zero-shot learning in music genre classification. In our ongoing work, we are applying our approach to a number of music information retrieval tasks.

## References

- Bengio, Y., Lamblin, P., Popovici, D. and Larochelle, H. Greedy layer-wise training of deep networks. In Schölkopf, B., Platt, J.C., and Hoffman, T. (eds.), *Advances in Neural Information Processing Systems 19 (NIPS'06)*, pp.153–160, Vancouver, B.C., Canada, 2007. The MIT Press.
- Bertin-Mahieux, T., Eck, D., and Mandel, M. Automatic tagging of audio: The state-of-the-art. In Wang, W. (ed.), *Machine Audition: Principles, Algorithms and Systems*, chapter 14, pp. 334-352. IGI Global, Hershey, PA, 2010.
- Blei, D., Ng, A., and Jordan, I. Latent dirichlet allocation. *Journal of Machine Learning Research*, 3:993–1022, 2003.
- Bromley, J., Bentz, J. W., Bottou, L., Guyon, I., Lecun, Y., Moore, C., Säckinger, E., and Shah, R. Signature verification using a “Siamese” time delay neural network. *International Journal of Pattern Recognition and Artificial Intelligence*, 7(4):669–688, 1993.
- Chen, S., Moore, J. L., Turnbull, D., and Joachims, T. Playlist prediction via metric embedding. *Proceedings of the 18th ACM SIGKDD International Conference on Knowledge Discovery and Data Mining (KDD'12)*, pp.714-722, New York, NY, USA, 2012. ACM.
- Collobert, R., Weston, J., Bottou, L., Karlen, M., Kavukcuoglu, K., and Kuksa, P. Natural Language Processing (almost) from Scratch. *Journal of Machine Learning Research*, 12:2493–2537, 2011.
- Deerwester, S., Dumais, S. and Landauer, T. Indexing by latent semantic analysis. *Journal of the American Society for Information Science*, 41(6):pp.391–407, 1990.
- Ferrand, L. and New, B. Semantic and associative priming in the mental lexicon. In P. Bonin (ed.), *Mental lexicon: Some words to talk about words*, chapter 2, pp. 25–43. Nova Biomedical, New York, NY, USA, 2000.
- Frome, A., Corrado, G., Shlens, J., Bengio, S., Dean, J., Ranzato, M., and Mikolov, T. DeViSE : A deep visual-semantic embedding model. In Burges, C.J.C., Bottou, L., Welling, M., Ghahramani, Z., and Weinberger, K.Q. (eds.), *Advances in Neural Information Processing Systems 26 (NIPS'13)*, pp.2121-2129. Lake Tahoe, NV, USA. 2013.
- Harris, Z.S. Distributional structure. *Word-Journal of the international linguistic association*, 10(2-3): pp.146–162, 1954.
- Hinton, G. A practical guide to training restricted Boltzmann machines. Technical Report, Computer Science Department, University of Toronto, Toronto, Canada, 2010.
- Hofmann, T. Probabilistic latent semantic indexing. *Proceedings of the 22nd ACM SIGIR conference on Research and development in information retrieval*. pp.50–57, New York, NY, USA, 1999. ACM.
- Kim, H., Scerri, S., Breslin, J., Decker, S., and Kim, H. The State of the Art in Tag Ontologies: A Semantic Model for Tagging and Folksonomies. *Dublin Core and Metadata Applications*. pp.128–137. Berlin, Germany. 2008. The Dublin Core Metadata Initiative.
- Law, E., Settles, B. and Mitchell, T. Learning to Tag from Open Vocabulary Labels. In Balcázar, J., Bonchi, F., Gionis, A., and Sebag, M. (eds.), *Proceedings of the 2010 European conference on Machine learning and knowledge discovery in databases (EMCL PKDD 2010)*. pp.211–226, Barcelona, Spain, 2010. Springer Berlin Heidelberg.
- Law, E., West, K., Mandel, M., Bay, M., and Downie, J. S. Evaluation of algorithms using games : the case of music tagging. *10th International Society for Music Information Retrieval Conference (ISMIR 2009)*, pp.387–392, Kobe, Japan, 2009.
- Lebret, R., LeGrand, J. and Collobert, R. Is deep learning really necessary for word embeddings? *Deep learning workshop, Advances in Neural Information Processing Systems 26 (NIPS'13)*. Lake Tahoe, NV, USA. 2013.
- Levy, M. and Sandler, M. Learning latent semantic models for music from social tags. *Journal of New Music Research*, 37(2):137–150, 2008.
- Maaten, L. and Hinton, G. Visualizing data using t-SNE. *Journal of Machine Learning Research*, 9:2579–2605, 2008.
- Mandel, M., Pascanu, R., Eck, D., Bengio, Y., Aiello, L., Schifanella, R., and Menczer, F. Contextual tag inference. *ACM Transactions on Multimedia Computing, Communications, and Applications*, 7S(1):1–18, 2011.

- D.Manning, C., Raghavan, P. and Schütze, H. *An Introduction to Information Retrieval*. Cambridge University Press, Online edition, 2009.
- Markines, B., Cattuto, C., Menczer, F., Benz, D., Hotho, A., and Stumme, G. Evaluating similarity measures for emergent semantics of social tagging. *Proceedings of the 18th international conference on World wide web (WWW'09)*. pp. 641-650. Madrid, Spain. 2009. ACM Press.
- Marques, G., Domingues, M.A., Langlois, T. and Gouyon, F. Three current issues in music autotagging. *12th International Society for Music Information Retrieval Conference (ISMIR 2011)*, pp.795–800. Miami, Florida, USA. 2011.
- Mikolov, T., Corrado, G., Chen, K. and Dean, J. Efficient estimation of word representations in vector space. *International Conference on Learning Representations (ICLR)*. Scottsdale, Arizona, USA. 2013.
- Mikolov, T., Karafiát, M., Burget, L., Cernocký, J., and Khudanpur, S. Recurrent neural network based language model. In T. Kobayashi, K. Hirose and S. Nakamura (eds.), *11th Annual Conference of the International Speech Communication Association*, pp.1045–1048. Makuhari, Chiba, Japan. 2010. ISCA.
- Miotto, R. and Lanckriet, G. A generative context model for semantic music annotation and retrieval. *IEEE Transactions on Audio, Speech, and Language Processing*, 20(4): pp.1096–1108, 2012.
- Ramage, D., Hall, D., Nallapati, R. and Manning, C.D. Labeled LDA: A supervised topic model for credit attribution in multi-labeled corpora. In P. Koehn and R. Mihalcea (eds.), *Proceedings of the 2009 Conference on Empirical Methods in Natural Language Processing: Volume 1*, pp.248–256. Singapore. 2009. ACM.
- Serra, X. et al.. *Roadmap for Music Information ReSearch (MIReS)*. The MIReS Consortium. 2013.
- Singhal, A. Modern information retrieval : A brief overview. *IEEE Data Engineering Bulletin*, 24: pp.35–43, 2001.
- Smeulders, A., Worring, M., Santini, S., Gupta, A., and Jain, R. Content-based image retrieval at the end of the early years. *IEEE Transactions on Pattern Analysis and Machine Intelligence*, 22(12): pp.1349–1380, 2000.
- Teh, W., Michael, I., Beal, M. and Blei, D. Hierarchical Dirichlet Processes. *Journal of the american statistical association*, 101(476), 2006.
- Turnbull, D., Barrington, L., Lanckriet, G. and Yazdani, M. Combining audio content and social context for semantic music discovery. *Proceedings of the 32nd international ACM SIGIR conference on Research and development in information retrieval (SIGIR'09)*, pp.387-394. Boston, MA, USA. 2009. ACM.
- Turnbull, D., Barrington, L., Torres, D. and Lanckriet, G. Towards musical query-by-semantic-description using the CAL500 data set. *Proceedings of the 30th annual international ACM SIGIR conference on Research and development in information retrieval (SIGIR'07)*, pp.439-446. Amsterdam; Netherlands. 2007. ACM.
- Wang, J., Anguera, X., Chen, X. and Yang, D. Enriching music mood annotation by semantic association reasoning. *2010 IEEE International Conference on Multimedia and Expo*, pp.1445–1450. Singapore. 2010. IEEE.
- Weston, J., Bengio, S. and Hamel, P. Multi-tasking with joint semantic spaces for large-scale music annotation and retrieval. *Journal of New Music Research*, 40(4): pp.337–348, 2011.

# Learning Contextualized Music Semantics from Tags via a Siamese Network: Supplementary Materials

In these supplementary materials, we present the technical details of the derivation of our learning algorithms, practical issues in learning, details on experimental settings and additional experimental results. The same notation system in the main text is used in these materials.

## A. Learning Algorithm Derivation

To minimize the loss functions for learning, we apply stochastic back propagation for parameter estimation. This actually means minimizing the cost function of the entire network using examples from the training data. The optimization task is performed iteratively by performing parameter movement along the partial derivative towards minimizing the cost.

### A.1. Sparse Auto-encoder Learning

We initialize the different layers by layer-wise greed training of sparse auto-encoders. An auto encoder is a neural network consisting of input, hidden and output layers. The basic purpose of this network is to reconstruct its input on the output.

Let  $\mathbf{x}$  be an input vector. The hidden layer's output is given by:

$$\mathbf{z}_1(\mathbf{x}) = \mathbf{f}(W_1\mathbf{x} + \mathbf{b}_1),$$

where  $W_1$  and  $\mathbf{b}_1$  are the encoding weights and biases, respectively, and  $\mathbf{f}(\cdot)$  is the hyperbolic tangent function used in our experiments.

The corresponding output is given by:

$$\tilde{\mathbf{x}}(\mathbf{x}) = \mathbf{f}(W_2\mathbf{z}_1(\mathbf{x}) + \mathbf{b}_2),$$

where  $W_2, \mathbf{b}_2$  are the decoding weights and biases, respectively.

The objective of the training is minimizing the following loss:

$$\mathcal{L}_A(\mathbf{x}; \Theta) = \|\tilde{\mathbf{x}}(\mathbf{x}) - \mathbf{x}\|_2^2 + \alpha\mathcal{R}.$$

$\mathcal{R}$  is a regularizer that is used to induce favorable representations. Sparsity of the hidden output is favored in our case. This is achieved by penalizing the magnitude of the hidden layer's output regardless of the sign.

$$\mathcal{R} = \sum_{q=1}^Q (\mathbf{z}_{1q}(\mathbf{x}) + \epsilon)^2,$$

where  $Q$  is the total number of neurons in the hidden layer.

The overall cost, in terms of all the dataset, is averaged over all the examples.

$$\mathcal{L}_A(X; \Theta) = \sum_{k=1}^K (\|\tilde{\mathbf{x}}(\mathbf{x}_k) - \mathbf{x}_k\|_2^2) + \alpha \sum_{k=1}^K \left( \sum_{q=1}^Q (\mathbf{z}_{1q}(\mathbf{x}_k))^2 + \epsilon \right)$$

Hence we achieve

$$\frac{\partial \mathcal{L}_A(X; \Theta)}{\partial \tilde{\mathbf{x}}} = 2 \sum_{k=1}^K \|\tilde{\mathbf{x}}(\mathbf{x}_k) - \mathbf{x}_k\|_2,$$

and

$$\frac{\partial \mathcal{R}}{\partial \mathbf{z}_1} = 2 \sum_{k=1}^K \left( \sum_{q=1}^Q \mathbf{z}_{1q}(\mathbf{x}_k) \right).$$

Let  $\nabla f(x)$  be the gradient of the hyperbolic function given input  $x$ . We have

$$\nabla f(x) = \frac{\partial f(x)}{\partial x} = \nabla \tanh(x) = 1 - (\tanh(x))^2$$

We use the chain rule to obtain the derivatives with respect to a specific parameter as follows:

$$\begin{aligned} \frac{\partial \mathcal{L}_A(X; \Theta)}{\partial W_2} &= \frac{\partial \mathcal{L}_A(X; \Theta)}{\partial \tilde{x}} \cdot \frac{\partial \tilde{x}}{\partial W_2} = 2 \sum_{k=1}^K ((\tilde{x}(\mathbf{x}_k) - \mathbf{x}_k) \cdot \nabla f(W_2 \mathbf{z}_1(\mathbf{x}_k) + \mathbf{b}_2) \cdot \mathbf{z}_1(\mathbf{x}_k)) \\ \frac{\partial \mathcal{L}_A(X; \Theta)}{\partial b_2} &= \frac{\partial \mathcal{L}_A(X; \Theta)}{\partial \tilde{x}} \cdot \frac{\partial \tilde{x}}{\partial b_2} = 2 \sum_{k=1}^K ((\tilde{x}(\mathbf{x}_k) - \mathbf{x}_k) \cdot \nabla f(W_2 \mathbf{z}_1(\mathbf{x}_k) + \mathbf{b}_2)) \\ \frac{\partial \mathcal{L}_A(X; \Theta)}{\partial W_1} &= \frac{\partial \mathcal{L}_A(X; \Theta)}{\partial \tilde{x}} \cdot \frac{\partial \tilde{x}}{\partial z_1} \cdot \frac{\partial z_1}{\partial W_1} + \alpha \frac{\partial \mathcal{R}}{\partial z_1} \frac{\partial z_1}{\partial W_1} = \\ & 2 \sum_{k=1}^K ((\tilde{x}(\mathbf{x}_k) - \mathbf{x}_k) \cdot \nabla f(W_2 \mathbf{z}_1(\mathbf{x}_k) + \mathbf{b}_2) \cdot W_2 \cdot \nabla f(W_1 \mathbf{x}_k + \mathbf{b}_1) \cdot \mathbf{x}_k) \\ & + 2\alpha \sum_{k=1}^K \left( (\sum_{q=1}^Q \mathbf{z}_{1q}(\mathbf{x}_k)) \cdot \nabla f(W_1 \mathbf{x}_k + \mathbf{b}_1) \cdot \mathbf{x}_k \right) \\ \frac{\partial \mathcal{L}_A(X; \Theta)}{\partial b_1} &= \frac{\partial \mathcal{L}_A(X; \Theta)}{\partial \tilde{x}} \cdot \frac{\partial \tilde{x}}{\partial z_1} \cdot \frac{\partial z_1}{\partial b_1} + \alpha \frac{\partial \mathcal{R}}{\partial z_1} \frac{\partial z_1}{\partial b_1} = \\ & 2 \sum_{k=1}^K ((\tilde{x}(\mathbf{x}_k) - \mathbf{x}_k) \cdot \nabla f(W_2 \mathbf{z}_1(\mathbf{x}_k) + \mathbf{b}_2) \cdot W_2 \cdot \nabla f(W_1 \mathbf{x}_k + \mathbf{b}_1)) \\ & + 2\alpha \sum_{k=1}^K \left( (\sum_{q=1}^Q \mathbf{z}_{1q}(\mathbf{x}_k)) \cdot \nabla f(W_1 \mathbf{x}_k + \mathbf{b}_1) \right) \end{aligned} \quad (\text{A.1})$$

Assembling the derivatives leads to the update rule:  $\Theta_{new} = \Theta_{old} - \eta \cdot \frac{\partial \mathcal{L}_A(X; \Theta)}{\partial \Theta}$ .

The sparse auto-encoder is employed to initialize a component network recursively where each layer is trained based on the output of its previous layer all the way until a pre-specified number of layers are achieved.

## A.2. Component Network Learning for Prediction

As defined in the main text in Eq.(3), the prediction loss is re-written as

$$\mathcal{L}_P(X; \Theta) = -\frac{1}{2K|\Gamma|} \sum_{k=1}^K \mathcal{L}_P(\mathbf{x}_k; \Theta),$$

Where

$$\mathcal{L}_P(\mathbf{x}_k; \Theta) = \sum_{i=1}^{|\Gamma|} (\kappa_k (1 + y_{ki}) \log(1 + \hat{y}_{ki}) + (1 - \kappa_k) (1 - y_{ki}) \log(1 - \hat{y}_{ki})).$$

Here,  $\hat{y}_{ki}$  and  $y_{ki}$  represent the prediction and its true label related to tag  $i$  in example  $k$ , respectively.  $|\Gamma|$  is the total number of tags in the training dataset.  $\kappa_k$  is a constant per example that emphasizes the cost of a false negative error.

By applying the chain rule, we have

$$\frac{\partial \mathcal{L}_P(X; \Theta)}{\partial x} = \frac{1}{K} \sum_{k=1}^K \left( \frac{\partial \mathcal{L}_P(\mathbf{x}_k; \Theta)}{\partial \hat{\mathbf{y}}_k} \cdot \frac{\partial \hat{\mathbf{y}}_k}{x} \right),$$

where  $\hat{\mathbf{y}}_k$  is the output vector of prediction, a collective notation of all  $\hat{y}_{ki}$ , also  $\cdot$  operator is the element wise multiplication. We have

$$\begin{aligned} \frac{\partial \mathcal{L}_P(\mathbf{x}_k; \Theta)}{\partial \hat{\mathbf{y}}_k} &= \frac{-1}{2|\Gamma|} \sum_{i=1}^{|\Gamma|} \left( \kappa_k \frac{1+y_{ki}}{1+\hat{y}_{ki}} \cdot \frac{\partial y_{ki}}{\partial \hat{y}_{ki}} - (1 - \kappa_k) \frac{1-y_{ki}}{1-\hat{y}_{ki}} \cdot \frac{\partial y_{ki}}{\partial \hat{y}_{ki}} \right) \\ &= \frac{-1}{2|\Gamma|} \left( \kappa_k \frac{1+y_k}{1+\hat{y}_k} - (1 - \kappa_k) \frac{1-y_k}{1-\hat{y}_k} \right), \end{aligned}$$

where  $\frac{1+y}{1+\hat{y}}$  and  $\frac{1-y}{1-\hat{y}}$  are the collective notation of  $\frac{1+y_{ki}}{1+\hat{y}_{ki}}$  and  $\frac{1-y_{ki}}{1-\hat{y}_{ki}}$  with the element-wise division.

Let  $\frac{\partial \mathcal{L}_P(\mathbf{x}_k; \Theta)}{\partial \hat{\mathbf{y}}}$  be the matrix formed by stacking all training  $\frac{\partial \mathcal{L}_P(\mathbf{x}_k; \Theta)}{\partial \hat{\mathbf{y}}_k}$  and  $\mathbf{z}_{H-1}(X)$  be the matrix formed by stacking all  $\mathbf{z}_{H-1}(\mathbf{x}_k)$ . The back propagation starts at the top layer with the partial of the cost on the last layer's parameters given by

$$\begin{aligned} \frac{\partial \mathcal{L}_P(X; \Theta)}{\partial W_H} &= \frac{1}{K} \sum_{k=1}^K \left( \frac{\partial \mathcal{L}_P(\mathbf{x}_k; \Theta)}{\partial \hat{\mathbf{y}}_k} \cdot \nabla \mathbf{f}(W_H \mathbf{z}_{H-1}(\mathbf{x}_k) + \mathbf{b}_H) \cdot \frac{\partial (W_H \times \mathbf{z}_{H-1}(\mathbf{x}_k) + \mathbf{b}_H)}{W_H} \right) \\ &= \frac{1}{K} \left( \frac{\partial \mathcal{L}_P(\mathbf{x}_k; \Theta)}{\partial \hat{\mathbf{y}}} \cdot \nabla \mathbf{f}(W_H \mathbf{z}_{H-1}(X) + \mathbf{b}_H) \right) * (\mathbf{z}_{H-1}(X))^T, \\ \frac{\partial \mathcal{L}_P(X; \Theta)}{\partial b_H} &= \frac{1}{K} \sum_{k=1}^K \left( \frac{\partial \mathcal{L}_P(\mathbf{x}_k; \Theta)}{\partial \hat{\mathbf{y}}_k} \cdot \nabla \mathbf{f}(W_H \mathbf{z}_{H-1}(\mathbf{x}_k) + \mathbf{b}_H) \right) = \frac{1}{K} \left( \frac{\partial \mathcal{L}_P(\mathbf{x}_k; \Theta)}{\partial \hat{\mathbf{y}}} \cdot \nabla \mathbf{f}(W_H \mathbf{z}_{H-1}(X) + \mathbf{b}_H) \right), \end{aligned} \quad (\text{A.2})$$

where  $*$  is the matrix multiplication.

Derivatives regarding other layers are obtained by the successive use of the chain rule (i.e. standard back propagation):

$$\begin{aligned} \frac{\partial \mathcal{L}_P(X; \Theta)}{\partial W_h} &= \frac{\partial \mathcal{L}_P(X; \Theta)}{\partial (W_h \mathbf{z}_h(X) + \mathbf{b}_h)} \cdot \frac{\partial (W_h \mathbf{z}_h(X) + \mathbf{b}_h)}{\partial W_h}, \\ \zeta_h &= \zeta_{h+1} \cdot \frac{\partial (W_{h+1} \mathbf{z}_{h+1}(X) + \mathbf{b}_{h+1})}{\partial \mathbf{z}_{h+1}(X)} \cdot \frac{\partial \mathbf{z}_{h+1}(X)}{\partial (W_h \mathbf{z}_h(X) + \mathbf{b}_h)} = W_{h+1} * (\zeta_{h+1} \cdot \nabla \mathbf{f}(W_h \mathbf{z}_h(X) + \mathbf{b}_h)), \\ \frac{\partial (W_h \mathbf{z}_h(X) + \mathbf{b}_h)}{\partial W_h} &= \mathbf{z}_h(X), \\ \frac{\partial \mathcal{L}_P(X; \Theta)}{\partial b_h} &= \frac{\partial \mathcal{L}_P(X; \Theta)}{\partial (W_h \mathbf{z}_h(X) + \mathbf{b}_h)} \cdot \frac{\partial (W_h \mathbf{z}_h(X) + \mathbf{b}_h)}{\partial b_h}, \\ \frac{\partial (W_h \mathbf{z}_h(X) + \mathbf{b}_h)}{\partial b_h} &= \mathbf{1}. \end{aligned} \quad (\text{A.3})$$

Based on the derivatives obtained above, an update iteration in our learning algorithm consists of four steps:

- 1- Feed forward step: given some input batch  $X$  (at least one vector of input  $\mathbf{x}$ ), we feed forward through the network until we get corresponding output vectors  $\hat{\mathbf{Y}}$  (at least one vector of output  $\hat{\mathbf{y}}$ ).
- 2- Error calculation using the error function: which measures how the output deviates from the intended output for each example  $\mathcal{L}_P(X; \Theta)$ .
- 3- Feed backward step: where we go through the network in a backward fashion calculating the analytical derivative for each weight and bias parameters  $\frac{\partial \mathcal{L}_P(X; \Theta)}{\partial \Theta}$ .
- 4- Update all parameters using the update rule:  $\Theta_{new} = \Theta_{old} - \eta \frac{\partial \mathcal{L}_P(X; \Theta)}{\partial \Theta}$  where  $\eta$  is a learning rate.

### A.3. Siamese Network Learning

In the main text, we define the Siamese loss defined in Eq. (4) as follows:

$$\mathcal{L}_S(X^{(1)}, X^{(2)}; \Theta) = \sum_{k=1}^K \left( I_1 \left( E(x_k^{(1)}, x_k^{(2)}) - \beta \left( 1 - e^{-\frac{\lambda}{2} KL(x_k^{(1)}, x_k^{(2)})} \right) \right)^2 + I_2 \rho \left( E(x_k^{(1)}, x_k^{(2)}) - \beta \left( 1 - e^{-\frac{\lambda}{2} KL(x_k^{(1)}, x_k^{(2)})} \right) \right)^2 + I_3 \left( E(x_k^{(1)}, x_k^{(2)}) - \beta \right)^2 e^{-\frac{\lambda}{2} KL(x_k^{(1)}, x_k^{(2)})} \right).$$

Here  $E(x_k^{(1)}, x_k^{(2)})$  is the Euclidian distance between the embedding vectors of the two input examples  $x_k^{(1)}, x_k^{(2)}$ ; and  $KL(x_k^{(1)}, x_k^{(2)})$  is based on their contexts similarity (c.f. Sect. 4 in the main text).

It should be noted that as far as the derivative with respect to weights and biases is concerned,  $\beta \left( 1 - e^{-\frac{\lambda}{2} KL(x_k^{(1)}, x_k^{(2)})} \right)$  is constant. Moreover, this loss is not affected by any of the prediction layer weights. Thus,

$$\frac{\partial \mathcal{L}_S(X^{(1)}, X^{(2)}; \Theta)}{\partial W_H} = 0 \quad \text{and} \quad \frac{\partial \mathcal{L}_S(X^{(1)}, X^{(2)}; \Theta)}{\partial b_H} = 0.$$

As there are two copies of the same network, all the parameters are updated to the same by using their averaging derivatives after each back propagating iteration. As there is no interaction between the two component neural networks apart from the CE layer, we can write

$$\frac{\partial \mathcal{L}_S(X^{(1)}, X^{(2)}; \Theta)}{\partial \Theta} = \frac{1}{2} \left( \frac{\partial \mathcal{L}_S(X^{(1)}, X^{(2)}; \Theta)}{\partial CE(X^{(1)})} \cdot \frac{\partial CE(X^{(1)})}{\partial \Theta} + \frac{\partial \mathcal{L}_S(X^{(1)}, X^{(2)}; \Theta)}{\partial CE(X^{(2)})} \cdot \frac{\partial CE(X^{(2)})}{\partial \Theta} \right).$$

As the loss is symmetric in terms of the embedding vectors, we only provide the derivative for one component neural network. The other would be the same except the component index.

$$\frac{\partial \mathcal{L}_S(X^{(1)}, X^{(2)}; \Theta)}{\partial CE(X^{(1)})} = \frac{1}{K} \sum_{k=1}^K \frac{\partial \mathcal{L}_S(x_k^{(1)}, x_k^{(2)}; \Theta)}{\partial CE(x_k^{(1)})}$$

$$\begin{aligned} \frac{\partial \mathcal{L}_S(x_k^{(1)}, x_k^{(2)}; \Theta)}{\partial CE(x_k^{(1)})} &= 2I_1 \left( E(x_k^{(1)}, x_k^{(2)}) - \beta \left( 1 - e^{-\frac{\lambda}{2} KL(x_k^{(1)}, x_k^{(2)})} \right) \right) \cdot \frac{\partial E(x_k^{(1)}, x_k^{(2)})}{\partial CE(x_k^{(1)})} \\ &\quad + 2\rho I_2 \left( E(x_k^{(1)}, x_k^{(2)}) - \beta \left( 1 - e^{-\frac{\lambda}{2} KL(x_k^{(1)}, x_k^{(2)})} \right) \right) \cdot \frac{\partial E(x_k^{(1)}, x_k^{(2)})}{\partial CE(x_k^{(1)})} \\ &\quad + 2I_3 \left( (E(x_k^{(1)}, x_k^{(2)}) - \beta) de^{-\frac{\lambda}{2} KL(x_k^{(1)}, x_k^{(2)})} \right) \cdot \frac{\partial E(x_k^{(1)}, x_k^{(2)})}{\partial CE(x_k^{(1)})} \end{aligned}$$

Focusing on  $\frac{\partial E(x_k^{(1)}, x_k^{(2)})}{\partial CE(x_k^{(1)})}$ , we have

$$\frac{\partial E(x_k^{(1)}, x_k^{(2)})}{\partial CE(x_k^{(1)})} = \frac{\|CE(x_k^{(1)}) - CE(x_k^{(2)})\|_1}{E(x_k^{(1)}, x_k^{(2)})}; \quad E(x_k^{(1)}, x_k^{(2)}) = \|CE(x_k^{(1)}) - CE(x_k^{(2)})\|_2.$$

Effectively, we can now estimate the partial derivatives for the embedding layer's weights and biases (on one network):

$$\begin{aligned}
 \frac{\partial \mathcal{L}_S(x_k^{(1)}, x_k^{(2)}; \Theta)}{\partial W_{H-1}} &= \frac{1}{K} \sum_{k=1}^K \frac{\partial \mathcal{L}_S(x_k^{(1)}, x_k^{(2)}; \Theta)}{\partial \mathbf{CE}(x_k^{(1)})} \cdot \frac{\partial \mathbf{CE}(x_k^{(1)})}{\partial W_{H-1}} \\
 &= \frac{1}{K} \sum_{k=1}^K \left( \frac{\partial \mathcal{L}_S(x_k^{(1)}, x_k^{(2)}; \Theta)}{\partial \mathbf{CE}(x_k^{(1)})} \cdot \nabla \mathbf{f}(W_{H-1} \mathbf{z}_{H-2}(x_k^{(1)}) + \mathbf{b}_{H-1}) \right) \cdot \frac{\partial (W_{H-1} \mathbf{z}_{H-2}(x_k^{(1)}) + \mathbf{b}_{H-1})}{\partial W_{H-1}} \\
 &= \frac{1}{K} \left( \frac{\partial \mathcal{L}_S(x_k^{(1)}, x_k^{(2)}; \Theta)}{\partial \mathbf{CE}(x_k^{(1)})} \cdot \nabla \mathbf{f}(W_{H-1} \mathbf{z}_{H-2}(\mathbf{x}_k) + \mathbf{b}_{H-1}) \right) * \left( \mathbf{z}_{H-2}(x_k^{(1)}) \right)^T, \\
 \frac{\partial \mathcal{L}_S(x_k^{(1)}, x_k^{(2)}; \Theta)}{\partial \mathbf{b}_{H-1}} &= \frac{1}{K} \left( \frac{\partial \mathcal{L}_S(x_k^{(1)}, x_k^{(2)}; \Theta)}{\partial \mathbf{CE}(x_k^{(1)})} \cdot \nabla \mathbf{f}(W_{H-1} \mathbf{z}_{H-2}(\mathbf{x}_k) + \mathbf{b}_{H-1}) \right). \tag{A.4}
 \end{aligned}$$

The rest of the derivatives are obtained by back propagating the cost in a similar fashion to that described in the single component case. Back propagation equations are given in Eqs.(A.3).

Once all derivatives are ready in both component networks, we average them for each parameter and use their average to update the parameters in each component networks.

Based on the derivatives obtained above, an update iteration in our learning algorithm consists of four steps:

- 1- Feed forward step: given some input batch  $X$  consisting of pairs of input vectors to be fed through the network (at least two vectors of input  $\mathbf{x}^{(1)}, \mathbf{x}^{(2)}$ ), we feed forward the vectors of the pairs of examples through the corresponding component sub-network until we get the corresponding embedding vectors  $\mathbf{CE}(X^{(1)}), \mathbf{CE}(X^{(2)})$
- 2- Error calculation using the error function: which measures how the embedding deviates from the intended embedding for each pair of examples  $\mathcal{L}_S(X^{(1)}, X^{(2)}; \Theta)$ .
- 3- Feed backward step: where we go through each network in a backward fashion calculating the analytical derivative for each weight and bias parameter in each network which are averaged per parameters  $\frac{\partial \mathcal{L}_S(X^{(1)}, X^{(2)}; \Theta)}{\partial \Theta}$ .
- 4- Update all parameters using the update rule:  $\Theta_{new} = \Theta_{old} - \eta \frac{\partial \mathcal{L}_P(X; \Theta)}{\partial \Theta}$ , where  $\eta$  is a learning rate.

## B. Model Selection and Hyper-parameter Setting

Model selection is carried out via training the network using Stochastic Back Propagation (SBP). In this section we present the data and cost function use in SBP, as well as provide explanation for hyper parameter tuning.

### B.1. Hyper-parameter setting

In layer-wise training, we used the sparse autoencoder with derivatives given in Eq (A.1). the related sparsity parameter  $\alpha$  value is set empirically to 2.

Most hyper-parameters were decided using grid search. Some parameters are automatically set by the dataset, such as  $\kappa$  and the size of the output layer. Others, however, are either set empirically or by following intuitive rules. However, the scale factor  $\beta$  is set directly to allow maximum use of the space. Assume the embedding size is  $d$  (i.e. the number of hidden neurons in the CE layer). With the nonlinearity transfer function applied, each dimension has a continuous value in  $[-1, +1]$ . Therefore, the hypercube formed has a maximum diagonal length of  $2\sqrt{d}$ . We set  $\beta$  to be half of that, so that the maximum distance between two concepts will still fit within the space. For example, for 10 dimensional embedding,  $\beta \leftarrow \sqrt{10} \approx 3$ .

$\lambda$  is set by observing trends in the context distances given by the  $KL$  distance. When the distances are comparatively small (or close to each other), the sensitivity must be high and thus  $\lambda$  is set to be small. In our experiments we use values between 0.5 and 2.

The Siamese contribution parameter  $\alpha$  is set to a large value. That is because each component network would already be trained for prediction before the combination of the two component networks. Thus, imposing the Siamese cost would only have effect if it contribution to the cost is high. However, large  $\alpha$  value would disable the effect of the prediction cost causing errors in embedding. Our setting is  $\alpha = 1000$  for CAL500 and  $\alpha = 2000$  for MagTag5K.

Setting the learning rate is done empirically. We set the learning rate to the largest value that allows immediate cost descent and reduce this value after every 100 iterations.

### B.2. Model Selection

The range of reasonable depth and layer sizes was explored. The network could have a number of hidden layers of 1, 2, 3, or 4. Deeper than that is acceptable but we realized that training the deepest architecture (i.e. 4 hidden layers) did not improve the embedding results over the one with 3 hidden layers, which effectively is used. Moreover, the width of the layers (i.e. number of neurons per layer) is tested with values 75, 100, 150 or 200 and we realized that most sizes are performing similarly with a slight advantage in using 100 neurons. Our embedding space is assumed 10 dimensions. We did not formally evaluate other sizes. However, informal testing suggested that this size is good enough for the embedding of the used datasets. In the general case, this should be tuned.

The dataset is split into in-vocabulary and out-of-vocabulary tags for OOV experiments at the beginning. We randomly select a number of tags and reserve them along with any documents using them. Using the in-vocabulary tags and the remaining documents as our dataset, we split the dataset into three fold and perform 3-fold cross validation experiments. Each fold consists of two thirds of the documents for training and one third for testing. That is 335 training documents and 167 test documents per fold for CAL500, and 2519 training documents, 1307 test documents and 1160 OOV documents per fold for MagTag5K. In each fold, we can obtain positive examples from coupling the tags with contexts they appear in. Negative examples are obtained by coupling tags with contexts they do not appear in.

Given a set of training examples  $X$  formed by all the positive examples, we initialize the weights using layer-wise training of sparse auto encoders. The encoding weights and biases as initial parameters for the component neural network. Then using training examples we train the component neural network using the prediction cost given in Eq. (3) and derived in Eqs. (A.2). In each iteration the positive examples and equal number of negative examples are provided to the network and the weights of the network are updates as per update rules.

Once the single component network is fully trained, a copy is made it in order to form the Siamese architecture, which is then trained using the total cost given in Eq. (5) and its parts derived in Eqs. (A.2) and (A.4). In each iteration pairs of examples are sampled randomly from the dataset and provided to the network. The weights of the network are updates as per the update rules.

The resulting model is tested using the training and test documents in each fold. The evaluation results reported are aggregated from all fold testing.

### C. Prediction Performance of Our Proposed Neural Architecture

The proposed architecture was trained in two stages: in the first learning stage, the architecture is only trained to predict related tags starting from features of a tag and its local context. Here we would like to evaluate the prediction performance of a component network in the first stage and the Siamese network further, which should provide an additional insight into the understanding our proposed neural architecture.

One major drawback of the prediction loss as described is its lack of ability to handle OOV. Moreover, there is no clear relatedness defined. This mapping is then disrupted by the introduction of the Siamese cost. However, it is still useful to investigate the prediction ability in order to better understand the results and the architecture.

The prediction task can be evaluated in the same priming setting described in the main text. A query tag is coupled with a local context and fed forward through the architecture. We measure the prediction of each in-vocabulary tag and rank those tags based on their predicted value and the  $P@k$  results are only reported as it is sufficient for this investigation.

We compare the prediction results at the end of training of the first stage (Single Prediction) and at the end of training the second stage (Siamese Prediction) on CAL500 and MagTag5K. As the same priming evaluation criterion is used, we also compare them to the embedding results reported within the main text.

Table C.1 shows the results on CAL500. In general, the prediction performance of a single (Single Prediction) component network is comparable to its embedding performance (Single CE.) as those output comes from two adjacent layers (i.e. layers  $H$  and  $H - 1$ ) without considering further constraints over embedding. Once the Siamese cost is introduced, however, it is observed from Table C.1 that the accuracy of the embedding (Siamese CE) increases at the cost that the prediction accuracy (Siamese Prediction) decreases in both training and test.

Table C.2 reports the results on MagTag5K where the same can be observed but the prediction performance of Siamese is degraded abruptly once the Siamese loss is applied due to the sparse use of tags in this datasets. In fact, our intuition is more validated in the MagTag5K results. The density of CAL500 makes it easier to predict at higher accuracies. This is still true after fine-tuning the CAL500 architecture.

In summary, learning representation in our case entailed training a predictor of in-vocabulary tags before fine tuning the embedding. We have shown that the prediction layer in the single component architecture is still powerful in its ability of priming, yet not as powerful as the embedding. Moreover, the embedding representation is able to handle OOV tags and provide meaningful distances. During the fine-tuning of the architecture, we intentionally neglect the prediction accuracy in favour of improved embedding. This allows the architecture to learn the wanted semantics properly.

METHOD	TRAINING				TEST			
	@1	@2	@5	@10	@1	@2	@5	@10
SINGLE PREDICTION	87.40 ± 2.40	85.17 ± 2.12	81.60 ± 1.24	76.55 ± 0.84	75.87 ± 3.37	74.13 ± 3.32	70.76 ± 2.58	66.05 ± 2.71
SINGLE CE	100.00 ± 0.00	88.20 ± 0.80	79.48 ± 1.22	76.35 ± 1.21	100.00 ± 0.00	80.13 ± 1.18	67.24 ± 1.86	62.10 ± 2.28
SIAMESE PREDICTION	73.93 ± 8.17	70.87 ± 6.81	65.89 ± 5.35	61.23 ± 5.62	60.67 ± 4.29	58.37 ± 3.59	55.79 ± 3.17	51.51 ± 3.49
SIAMESE CE	100.00 ± 0.00	91.57 ± 1.40	84.89 ± 1.24	82.73 ± 1.56	100.00 ± 0.00	80.40 ± 1.45	67.51 ± 2.30	63.01 ± 2.43

Table C.1. Priming accuracy (%) of single and Siamese models at different levels on CAL500.

METHOD	TRAINING				TEST			
	@1	@2	@5	@10	@1	@2	@5	@10
SINGLE PREDICTION	76.20 ± 5.72	71.97 ± 3.81	59.97 ± 4.21	42.93 ± 2.41	72.27 ± 4.12	66.63 ± 4.82	54.79 ± 4.42	38.09 ± 3.44
SINGLE CE	100.00 ± 0.00	86.23 ± 0.21	71.65 ± 0.60	49.57 ± 1.70	100.00 ± 0.00	82.83 ± 2.59	64.69 ± 6.08	43.50 ± 4.46
SIAMESE PREDICTION	32.40 ± 1.83	29.30 ± 2.82	25.29 ± 4.08	22.33 ± 2.34	28.40 ± 2.69	26.33 ± 1.38	22.29 ± 2.09	19.74 ± 1.67
SIAMESE CE	100.00 ± 0.00	88.33 ± 0.50	75.49 ± 1.72	54.14 ± 1.34	100.00 ± 0.00	82.70 ± 1.57	67.57 ± 3.42	46.30 ± 2.55

Table C.2. Priming accuracy (%) of single and Siamese models at different levels on MagTag5K.

## D. Experimental Setting of Other Models in Comparison

As discussed in Sect.5 of the main text, we compare our approach to a number of music semantic learning models in terms of the Priming task. In each model, tags are represented somehow and then a relatedness measure is applied to the tags in context. In global relatedness models, the context is ignored in any query. In this section, we provide details regarding how to represent tags and measure similarity in each used model in our experiments.

### D.1. Parameter Setting

In LSI, each tag is represented as set of values resulting from performing SVD on the re-weighted document-tag matrix. The document-tag matrix can be re-weighting in three ways:

- *tf*: the binary document-tag relatedness is kept (c.f. Sect. 3 of the main text ).
- *tfidf*: the *tfidf* weighting scheme is described in Sect. 3 of the main text.
- *PMI*: the point-wise mutual information that measures the lack of compatibility of the distribution of tag and that of a document. Hence, it highlights rare events, such as very short documents or very rare tags used.

The above measures are used for other models as well.

After the re-weighting of the document-tag matrix, the resulting matrix is decomposed using SVD, which effectively yields a lower dimensionality representation for each tag. These representations are used in the priming task.

For evaluating the priming ability, we query the model with tags in context. However, the context is ignored in this case and related tags are primed based on their Euclidian or cosine distance to the query tag. Among the different results achieved by all the settings, we report only those of the highest accuracy. Consequently, the PMI results are reported for CAL500 and *tfidf* results are reported for MagTag5K. In both cases, priming using the cosine measure led to the best performance.

In PCA, similar document-tag re-weighting to that of LSI is carried out. Once the re-weighted document-tag matrix is obtained, we measure the global relatedness between any pair of tags by considering their usage vector (c.f. Sect. 3 of the main text) and measuring the distance between the pair of usage vectors using one of five possible measures:

- Dot product: the usage vectors are simply multiplied.
- Cosine: the cosine distance between the usage vectors is used.
- KL-Divergence: the KL divergence, assuming that the usage vector is a multinomial distribution.
- Hellinger-Distance: the Hellinger-Distance, assuming that the usage vector is a multinomial distribution.
- Mutual Information: the Mutual Information, assuming that the usage vector is a multinomial distribution.

The result of this process is a tag-to-tag relatedness matrix. The rows of this matrix reflect the usage patterns of each tag and its columns represent used tags which can be seen as features of those tags; a row forms a feature vector for a tag. For this reason, we use PCA to reduce the dimensionality of the tag representation acquired by the previous process. The lower dimensionality is set to 10 in order to match our own architecture's embedding size.

The evaluation of this process proceeds by measuring cosine or Euclidian distance in the 10-D dimensional space. Among the different results achieved by all the settings, we report only those of the highest accuracy. Consequently, the *PMI+dot-product* results are reported for CAL500 and *tfidf+KL-divergence* results are reported for MagTag5K. In both cases, priming using the Euclidian distance led to the best performance.

For the *InfoTh*, tags are first represented in a similar manner to PCA. Then we apply the smoothing by exploring the parameter space. That is, for each original PCA setting, we have to do grid search over the space of smoothing parameters in search for best performance. The smoothing parameters tested are as follows  $K \in \{1,3,5,7,9\}$  and  $\alpha \in$

{0.1,0.2,0.3,0.4,0.5} generating a total of 375 possible tag representations per dataset. We evaluate all in search of the best possible setting.

When the tags are represented in a 10-D representational space, we observe a substantial decrease in accuracy. Therefore, we abandoned the dimension reduction step and instead used the high dimensionality representations (158 dimensions in CAL500 and 114 in MagTag5K). The evaluation of *InfoTh* proceeds by measuring Euclidian, cosine or mutual information distance in the tag representation space. Among the different results achieved by all the settings, we report only those of the highest accuracy. Consequently, the *tfidf+product* ( $K = 9, \alpha = 0.1$ ) results are reported for CAL500 and *tfidf+cosine* ( $K = 9, \alpha = 0.2$ ) results are reported for MagTag5K. In both cases, priming using the mutual information led to the best performance.

The RBM model was trained by using the BoW representation directly. Each document is presented to the model independently and the model is train using the Contrastive Divergence (CD) algorithm. During the test, we clamp one tag ‘on’ and perform sampling chains a large number of times. Eventually, we average the activation of each visible neuron and assume that the co-activation encodes relatedness.

Similarly, the C-RBM is trained using the BoW representation and the one-hot representation of documents as the condition (each training document is given its own neuron on the condition). The training is also done via the CD algorithm, and the same protocol used for the RBM was applied here for test apart from the sampling chain as the C-RBM takes the condition part into account.

Two natural language models are trained using the *word2vec* (<https://code.google.com/p/word2vec>) package. Continuous Skip-Gram (C-SG) and Continuous Bag-of-words (C-BoW) used different window sizes where we also shuffled the tags in different orders. During training, each tag was given its lower dimensional representation based on its syntactic use by considering a number of ‘neighboring’ tags. The evaluation of this process proceeds by measuring cosine or Euclidian distance in the lower dimensionality space. Among the different results achieved by all the settings, we report only those of the highest accuracy. Consequently, for C-BoW  $|Window|=1$  results are reported for CAL500 and  $Window=2$  for MagTag5K. On the other hand, for C-SG  $Window=2$  results are reported for CAL500 and  $Window=1$  for MagTag5K. In all cases, priming using the cosine distance led to the best performance. (c.f. Sect. E of this document for more details regarding the accuracy of two language models).

We also evaluated p-LSA and LDA. The tags are represented as statistical events and probability follows a well-designed distribution that is learnt from the data. After training, the relatedness between a pair of tags  $\tau_1$  and  $\tau_2$  can be approximated under a specific topic distribution as (assuming equal prior for all the tags):

$$\begin{aligned} KL(\tau_1, \tau_2) &= \sum_{c=1}^{|\Phi|} (p(\theta_c|\tau_1) - p(\theta_c|\tau_2)) \cdot \left( \log \left( \frac{p(\theta_c|\tau_1)}{p(\theta_c|\tau_2)} \right) \right) \\ &= \sum_{c=1}^{|\Phi|} p(\theta_c) \left( \frac{p(\tau_1|\theta_c)}{p(\tau_1)} - \frac{p(\tau_2|\theta_c)}{p(\tau_2)} \right) \cdot \left( \log \left( \frac{p(\tau_2) \cdot p(\tau_1|\theta_c)}{p(\tau_1) \cdot p(\tau_2|\theta_c)} \right) \right) \\ &= \frac{1}{p(\tau)} \sum_{c=1}^{|\Phi|} p(\theta_c) (p(\tau_1|\theta_c) - p(\tau_2|\theta_c)) \cdot \left( \log \left( \frac{p(\tau_1|\theta_c)}{p(\tau_2|\theta_c)} \right) \right). \end{aligned}$$

The random model simply returned a random list as the priming results for a query tag.

## D.2. Embedding space visualization

Along with the visualization provided in Sect.5 of the main text, we explore the co-location ability of a model by looking into the embedding of a document regarding one song.

For the song, “sweat machine”, we applied different models to project all the available tags from CAL500. For visualization, we use the unsupervised t-SNE as a dimensionality reduction method to project the semantic embedding representations of tags generated by different models onto a 2D space as shown in Fig. D.1 where each plot corresponds to one model. The tags can be seen as two types: the related tags used in the document in question, such as Emotional, Passionate, Light Playful, Positive Optimistic, Touching Loving, Alternative, Rock, Drum Set, Positive Feelings, Recorded and Studying; and the non-related tags which are the rest of the tags in CAL500. In Fig. D.1, we denote the related tags with circle and the non-related tags with cross, respectively.

The different models lead to different representational schemes in embedding. For example, PCA embedding is context-free and hence a tag always has the same representation in its embedding space. The representation of a document can be achieved by collectively using representations of all tags over the embedding space. This is evident from the PCA plot in Fig. D.1. Similarly, C-SG and C-BoW have the same global-relatedness-only embedding. This can also be observed from their corresponding plots in Fig. D.1. On the other hand, LDA is context-dependent as it assumes that the tag-to-tag relatedness differs under different topics. Regardless of the distance measures used, the plot on LDA does not yield a clear semantic grouping on related tags. Instead several clusters of related tags seem to emerge but less relevant to semantic meaning.

In contrast to those models, ours co-locate the related tags in context. It is evident that the Single CE can group the related tags together to a great degree. Thanks to the used Siamese cost, Siamese CE clearly separates all related and non-related tags and, in particular, make all related tags co-located tightly in the embedding space. This visualization suggests that our proposed approach effectively captures the semantic meanings of all the tags used in the song.

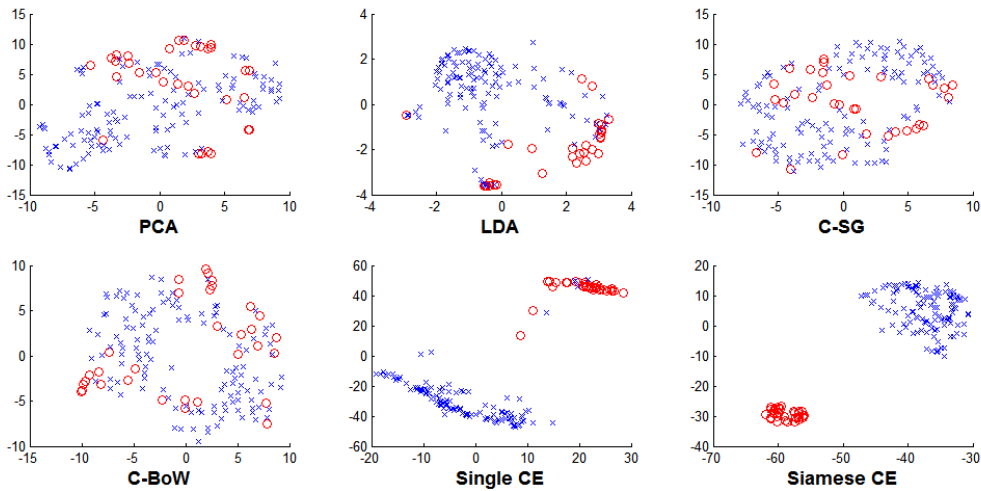


Figure D.1. The behavior of different semantic embedding on their 2-D projection.

## E. Further Experimental Results on Distributed Natural Language Models

Distributed language models rely on the syntactic structures found in language; the meaning of a word is inferred based on its order as well as the accompanying words. However, tag collections do not have syntactic structures and tags can occur in any ‘order’ when describing a document, which may cause such language models to fail in dealing with data collections containing only tags.

In order to verify this hypothesis, we trained and tested two prominent distributed language models, i.e. Continuous Bag of Words (C-BoW) and Continuous Skip Gram (C-SG) in two different settings:

- Setting 1 (S1): we randomly ordered the tags in each document and train the model. In this case, a model is expected to learn information about the natural relationships present between tags.
- Setting 2 (S2): We assigned a pseudo-order on all the tags by designating one tag to be tag number 1, another tag to be tag number 2, etc. Tags in a document were sorted based on the pre-specified pseudo-order before training. In this case, a model may learn syntactic information as well as the wanted semantics.

In a model, the window size refers to the number of tags to be considered on each side of the focus tag (before or after). This is one of the most important parameters in a language model. In our situation, the window size should not be large as there are only a small number of tags in a document. As a result, we tested on different window sizes of 1-4 with both settings.

Test was carried out in a similar fashion to the priming explained in our experiments (c.f. Sect. 5 of the main text). The results on CAL500 and MagTag5K are listed in Tables E.1 and E.2. We also tabulated results of the Random and the PCA models for comparison. From Tables E.1 and E.2, it is observed that the priming accuracy sharply dropped at level 2 regardless of experimental settings. In the S2 setting, the window size seems irrelevant to the performance; the use of four different windows on CAL 500 led to the exact same embedding vectors as clearly shown in Table E.1. On the other hand, the S1 setting causes another problem for a larger window size; the larger the window size the lower the accuracy on training and testing as shown in Tables E.1 and E.2. It is observed that the C-SG with the window size of 1 in the S1 setting performs the best on both datasets in terms of MAP. This suggests that there is no syntactic structure in the tag collections, which is responsible for the failure of the language models in this experiment.

The PCA works on the tag-to-tag relatedness matrix and hence only captures pair-wise global relatedness without considering syntactic structures. However, its performance is much better than that of those language models, which further confirms our hypothesis that distributed language models are inapplicable to the contextualized semantic learning from tags.

In summary, it is evident from our experimental results that the current state-of-the-art distributed language models are not able to capture accurate contextualized music semantics from tags. This investigation actually helped us gain our motivation to formulate the problem on learning the contextualized music semantics from tags and to present a solution as presented in the main text.

## Learning Contextualized Music Semantics from Tags via a Siamese Network: Supplementary Materials

METHOD		TRAINING					TEST				
NAME	WINDOW	@1	@2	@5	@10	MAP	@1	@2	@5	@10	MAP
RANDOM		100 ± 0.00	58.15 ± 0.38	33.06 ± 0.15	24.69 ± 0.07	28.95 ± 0.06	100 ± 0.00	57.98 ± 0.17	33.11 ± 0.03	24.63 ± 0.11	29.00 ± 0.21
C-BOW (S1)	1	100 ± 0.00	69.52 ± 1.62	48.75 ± 1.50	40.27 ± 1.24	42.12 ± 1.06	100 ± 0.00	68.91 ± 1.59	47.76 ± 2.26	39.26 ± 1.68	41.2 ± 1.44
	2	100 ± 0.00	68.02 ± 1.57	47.43 ± 1.08	38.31 ± 0.83	40.44 ± 0.97	100 ± 0.00	67.85 ± 1.89	46.87 ± 1.93	37.60 ± 1.58	39.8 ± 1.47
	3	100 ± 0.00	66.40 ± 0.83	45.63 ± 2.00	37.19 ± 1.18	39.5 ± 1.06	100 ± 0.00	65.80 ± 0.18	44.89 ± 2.40	36.33 ± 2.25	38.77 ± 1.58
	4	100 ± 0.00	65.76 ± 1.33	46.65 ± 0.71	36.96 ± 0.77	39.54 ± 0.58	100 ± 0.00	65.39 ± 2.61	45.66 ± 2.68	36.12 ± 2.84	38.81 ± 2.07
C-SG (S1)	1	100 ± 0.00	69.94 ± 0.58	50.20 ± 0.91	40.89 ± 0.66	42.63 ± 0.65	100 ± 0.00	69.27 ± 0.39	49.38 ± 1.52	39.89 ± 1.67	41.73 ± 1.25
	2	100 ± 0.00	70.11 ± 1.52	49.04 ± 1.25	39.07 ± 1.45	41.22 ± 0.75	100 ± 0.00	69.76 ± 2.16	48.40 ± 1.20	38.24 ± 0.45	40.55 ± 0.49
	3	100 ± 0.00	66.57 ± 2.39	46.12 ± 1.63	36.80 ± 1.01	39.54 ± 1.19	100 ± 0.00	66.11 ± 2.42	45.14 ± 2.19	35.98 ± 1.70	38.81 ± 1.39
	4	100 ± 0.00	68.49 ± 2.49	46.21 ± 1.48	37.40 ± 1.38	40.23 ± 0.97	100 ± 0.00	68.14 ± 2.01	45.48 ± 0.58	36.63 ± 1.24	39.50 ± 0.63
C-BOW (S2)	1	100 ± 0.00	69.13 ± 1.95	46.28 ± 1.46	35.61 ± 1.57	37.93 ± 1.05	100 ± 0.00	68.63 ± 2.31	45.88 ± 1.08	35.37 ± 0.11	37.66 ± 0.17
	2	100 ± 0.00	69.13 ± 1.95	46.28 ± 1.46	35.61 ± 1.57	37.93 ± 1.05	100 ± 0.00	68.63 ± 2.31	45.88 ± 1.08	35.37 ± 0.11	37.66 ± 0.17
	3	100 ± 0.00	69.13 ± 1.95	46.28 ± 1.46	35.61 ± 1.57	37.93 ± 1.05	100 ± 0.00	68.63 ± 2.31	45.88 ± 1.08	35.37 ± 0.11	37.66 ± 0.17
	4	100 ± 0.00	69.13 ± 1.95	46.28 ± 1.46	35.61 ± 1.57	37.93 ± 1.05	100 ± 0.00	68.63 ± 2.31	45.88 ± 1.08	35.37 ± 0.11	37.66 ± 0.17
C-SG (S2)	1	100 ± 0.00	67.78 ± 0.87	47.63 ± 0.95	37.57 ± 0.98	39.35 ± 0.65	100 ± 0.00	67.47 ± 0.99	47.29 ± 1.04	37.01 ± 0.30	38.90 ± 0.37
	2	100 ± 0.00	67.78 ± 0.87	47.63 ± 0.95	37.57 ± 0.98	39.35 ± 0.65	100 ± 0.00	67.47 ± 0.99	47.29 ± 1.04	37.01 ± 0.30	38.90 ± 0.37
	3	100 ± 0.00	67.78 ± 0.87	47.63 ± 0.95	37.57 ± 0.98	39.35 ± 0.65	100 ± 0.00	67.47 ± 0.99	47.29 ± 1.04	37.01 ± 0.30	38.90 ± 0.37
	4	100 ± 0.00	67.78 ± 0.87	47.63 ± 0.95	37.57 ± 0.98	39.35 ± 0.65	100 ± 0.00	67.47 ± 0.99	47.29 ± 1.04	37.01 ± 0.30	38.90 ± 0.37
PCA		100 ± 0.00	<b>80.72 ± 0.71</b>	<b>65.21 ± 0.81</b>	<b>56.35 ± 0.72</b>	<b>55.39 ± 0.74</b>	100 ± 0.00	<b>79.78 ± 0.68</b>	<b>63.92 ± 0.96</b>	<b>54.89 ± 0.85</b>	<b>55.39 ± 0.74</b>

Table E.1. Priming accuracy (%) of Language models at different levels on CAL500.

METHOD		TRAINING					TEST				
NAME	WINDOW	@1	@2	@5	@10	MAP	@1	@2	@5	@10	MAP
RANDOM		100 ± 0.00	52.12 ± 0.08	23.35 ± 0.19	13.73 ± 0.11	47.90 ± 0.59	100 ± 0.00	52.06 ± 0.26	23.29 ± 0.30	13.71 ± 0.28	47.89 ± 1.20
C-BOW (S1)	1	100 ± 0.00	60.10 ± 0.89	36.04 ± 0.75	24.56 ± 0.83	57.07 ± 0.59	100 ± 0.00	60.16 ± 2.80	35.37 ± 3.40	23.87 ± 2.61	56.88 ± 1.63
	2	100 ± 0.00	61.13 ± 1.94	34.58 ± 1.30	23.31 ± 0.37	56.71 ± 0.61	100 ± 0.00	61.17 ± 3.36	34.12 ± 2.86	22.69 ± 2.58	56.47 ± 1.18
	3	100 ± 0.00	60.55 ± 0.08	34.04 ± 1.45	23.09 ± 0.31	56.28 ± 1.39	100 ± 0.00	60.57 ± 2.03	34.29 ± 3.69	22.97 ± 2.25	56.43 ± 1.58
	4	100 ± 0.00	60.55 ± 2.39	33.66 ± 1.78	23.05 ± 0.16	56.17 ± 1.58	100 ± 0.00	60.88 ± 3.01	33.43 ± 3.78	22.69 ± 2.47	56.19 ± 1.81
C-SG (S1)	1	100 ± 0.00	61.55 ± 1.59	35.60 ± 1.07	24.01 ± 0.36	57.54 ± 1.08	100 ± 0.00	61.59 ± 4.74	35.18 ± 4.40	23.32 ± 3.15	57.34 ± 2.95
	2	100 ± 0.00	61.91 ± 1.87	33.43 ± 0.48	22.50 ± 0.77	56.55 ± 0.89	100 ± 0.00	61.18 ± 3.41	33.05 ± 3.03	22.35 ± 2.22	56.17 ± 1.78
	3	100 ± 0.00	60.79 ± 0.71	33.40 ± 1.52	21.86 ± 0.84	55.94 ± 0.53	100 ± 0.00	61.05 ± 1.58	33.52 ± 3.10	21.79 ± 2.73	55.97 ± 1.27
	4	100 ± 0.00	56.73 ± 1.30	31.10 ± 0.82	21.45 ± 1.01	53.53 ± 1.67	100 ± 0.00	57.30 ± 2.03	31.54 ± 2.64	21.77 ± 2.47	53.99 ± 1.46
C-BOW (S2)	1	100 ± 0.00	60.37 ± 0.68	34.90 ± 2.09	24.38 ± 1.33	56.53 ± 0.41	100 ± 0.00	59.73 ± 2.08	33.72 ± 2.20	23.34 ± 2.00	55.7 ± 1.06
	2	100 ± 0.00	60.26 ± 1.15	33.30 ± 0.71	22.98 ± 0.35	55.81 ± 1.15	100 ± 0.00	59.54 ± 2.91	32.67 ± 3.30	22.34 ± 2.9	55.31 ± 1.55
	3	100 ± 0.00	59.40 ± 1.67	33.92 ± 0.67	22.51 ± 1.14	55.51 ± 0.23	100 ± 0.00	59.20 ± 2.75	33.16 ± 2.46	21.92 ± 1.36	55.17 ± 1.21
	4	100 ± 0.00	60.05 ± 1.68	33.61 ± 0.92	22.37 ± 0.63	56.07 ± 0.52	100 ± 0.00	60.09 ± 2.84	33.03 ± 1.48	21.87 ± 1.68	55.75 ± 1.68
C-SG (S2)	1	100 ± 0.00	60.02 ± 2.01	34.20 ± 0.53	23.82 ± 0.88	56.36 ± 1.27	100 ± 0.00	60.24 ± 3.96	33.98 ± 2.74	23.40 ± 3.19	56.27 ± 1.55
	2	100 ± 0.00	60.58 ± 0.95	33.34 ± 1.41	22.99 ± 0.60	55.90 ± 0.95	100 ± 0.00	59.98 ± 2.80	32.81 ± 3.19	22.22 ± 2.60	55.43 ± 1.50
	3	100 ± 0.00	59.07 ± 1.03	32.68 ± 0.77	22.12 ± 0.75	54.96 ± 0.52	100 ± 0.00	58.84 ± 2.68	31.96 ± 1.87	21.47 ± 2.21	54.51 ± 0.93
	4	100 ± 0.00	59.64 ± 0.88	32.53 ± 1.52	21.42 ± 1.76	55.10 ± 0.90	100 ± 0.00	59.25 ± 1.39	31.82 ± 2.25	20.70 ± 0.92	54.62 ± 1.73
PCA		100 ± 0.00	<b>69.15 ± 0.70</b>	<b>41.63 ± 1.29</b>	<b>28.28 ± 1.05</b>	<b>62.86 ± 0.33</b>	100 ± 0.00	<b>68.26 ± 2.36</b>	<b>40.59 ± 2.67</b>	<b>27.46 ± 1.99</b>	<b>62.00 ± 1.08</b>

Table E.2. Priming accuracy (%) of Language models at different levels on MagTag5K.